Crystallographic, Molecular Modeling, and Biophysical Characterization of the Valine$^{\beta 67}$ (E11) → Threonine Variant of Hemoglobin[†,‡]

Igor Pechik,[§,||] Xinhua Ji,[§] Krzysztof Fidelis,[⊥,▽] Michael Karavitis,[#] John Moult,[§] William S. Brinigar,[°] Clara Fronticelli,[*,#] and Gary L. Gilliland[*,§]

Center for Advanced Research in Biotechnology of the University of Maryland Biotechnology Institute and National Institute of Standards and Technology, 9600 Gudelsky Drive, Rockville, Maryland 20850, Department of Biochemistry, University of Maryland Medical School, 108 N. Greene Street, Baltimore, Maryland 21201, Department of Chemistry, Temple University, Philadelphia, Pennsylvania 19122, Biology and Biotechnology Research Program, Lawrence Livermore National Laboratory, Livermore, California 94551

Received August 22, 1995; Revised Manuscript Received December 5, 1995[⊗]

ABSTRACT: The crystal structure of the mutant deoxyhemoglobin in which the β-globin Val^{67}(E11) has been replaced with threonine [Fronticelli et al. (1993) *Biochemistry 32*, 1235−1242] has been determined at 2.2 Å resolution. Prior to the crystal structure determination, molecular modeling indicated that the Thr^{67}(E11) side chain hydroxyl group in the distal β-heme pocket forms a hydrogen bond with the backbone carbonyl of His^{63}(E7) and is within hydrogen-bonding distance of the N$^{\delta}$ of His^{63}(E7). The mutant crystal structure indicates only small changes in conformation in the vicinity of the E11 mutation confirming the molecular modeling predictions. Comparison of the structures of the mutant β-subunits and recombinant porcine myoglobin with the identical mutation [Cameron et al. (1993) *Biochemistry 32*, 13061−13070] indicates similar conformations of residues in the distal heme pocket, but there is no water molecule associated with either of the threonines of the β-subunits. The introduction of threonine into the distal heme pocket, despite having only small perturbations in the local structure, has a marked affect on the interaction with ligands. In the oxy derivative there is a 2-fold decrease in O_2 affinity [Fronticelli et al. (1993) *Biochemistry 32*, 1235−1242], and the rate of autoxidation is increased by 2 orders of magnitude. In the CO derivative the IR spectrum shows modifications with respect to that of normal human hemoglobin, suggesting the presence of multiple CO conformers. In the nitrosyl derivative an interaction with the O$^{\gamma}$ atom of Thr^{67}(E11) is probably responsible for the 10-fold increase in the rate of NO release from the β-subunits. In the aquomet derivative there is a 6-fold decrease in the rate of hemin dissociation suggesting an interaction of the Fe-coordinated water with the O$^{\gamma}$ of Thr^{67}(E11).

Structural features of oxygen binding to hemoglobin and myoglobin have been known since the high-resolution structures of the unliganded and liganded proteins were determined (Shanaan, 1983; Fermi et al., 1984). Oxygen and other ligands bind to the Fe in the distal heme pockets of myoglobin and hemoglobin. The wall of the distal heme pocket forms an effective barrier for sequestering the heme Fe from the bulk solvent associated with the surface of the protein. For both hemoglobin and myoglobin, the ligand cannot gain entrance to the distal heme pocket(s) unless there is a reorientation of the His(E7) side chain or that of another distal heme pocket amino acid residue. This was first recognized by Perutz and Mathews (1966) in an early crystallographic study examining azide binding to methemoglobin.

Recombinant hemoglobin and myoglobin have been used extensively to investigate the molecular mechanism of ligand binding to the heme. A series of site-directed mutations that alter the size and polarity of amino acid residues associated with the distal heme pocket have been constructed and characterized (Nagai et al., 1987; Olson et al., 1988; Springer et al., 1989; Carver et al., 1990, 1991, 1992; Egeberg et al., 1990; Rohlfs et al., 1990; Smerdon et al., 1991; Tame et al., 1991; Cameron et al., 1993; Fronticelli, 1993). The primary focus of these studies has been the His(E7) and/or Val(E11), two residues that are directly associated with the ligand binding site. Mutation of His(E7) suggests that for α-globin and myoglobin the polar character of the histidine side chain rather than its size controls ligand entry into the heme pocket (Olson et al., 1988; Springer et al., 1989; Carver et al., 1990; Rohlfs et al., 1990). However, this is not true for the β-globin whose affinity for O_2 is not modified by substitutions at His(E7) (Nagai et al., 1987; Olson et al., 1988; Mathews et al., 1989).

Studies involving substitutions of Val(E11) show that increasing the volume of the amino acid side chain in the order of Ala to Val to Ile to Phe, causes a decrease in the

[†] This work was supported in part by PHS NIH Grant HLBI-48517 (C.F., G.G., J.M.), under the auspices of the DOE by LNL under Contract No. W-7405-Eng-48 (K.F.) and Laboratory Directed Research and Development Award 93-DI-003 (K.F.) and by the Research Incentive Fund, Temple University (W.S.B.).

[‡] The crystallographic coordinates for the deoxy structures of the natural and mutant hemoglobins reported here have been deposited in the Brookhaven Protein Data Bank and assigned the identifiers 2HHD and 1HDB, respectively.

* Address correspondence to these authors.

[§] Center for Advanced Research in Biotechnology.

[||] Participated in this work at CARB as a Guest Scientist from the V. A. Englehardt Institute of Molecular Biology, Russian Academy of Sciences, Moscow, Russia.

[⊥] Lawrence Livermore National Laboratory.

[▽] Previous address: Center for Advanced Research in Biotechnology, Rockville, MD 20850.

[#] University of Maryland, Medical School.

[°] Temple University.

[⊗] Abstract published in *Advance ACS Abstracts,* January 15, 1996.

0006-2960/96/0435-1935$12.00/0

association rate constant for a number of ligands that bind to myoglobin and α-subunits; however, these mutations have little effect on ligand association rates with β-subunits, except for Ile which sterically hinders the access of O_2 to the heme (Mathews et al., 1989). These data suggest a similarity between the distal heme pockets of myoglobin and of the α-subunits while the β-subunits seems to have a different stereochemical mechanism of ligand binding. The relevance of the polar character of the residue at position E11 has been investigated by replacing the conserved valine with isosteric threonine in porcine myoglobin (Cameron et al., 1993) and the β-globin of hemoglobin (Fronticelli et al., 1993). Although the substitutions have the effect of decreasing ligand affinity in both cases, the extent of this effect is different. In porcine myoglobin the O_2 and CO affinity of the mutant were decreased by 17- and 6-fold, respectively. The hemoglobin mutant has a 2-fold reduction in the affinities for both O_2 and CO. For both proteins, the reduced O_2 affinity is due to a decrease in the "on" rate while the reduced CO affinity is due to an increase in the "off" rate, suggesting a similarity in the spatial arrangement of the atoms of the heme pocket in the two proteins.

We report here the crystal structure determination at 2.2 Å resolution of the deoxy form of the mutant hemoglobin (βV67T)[1] in which the β-globin Val[67](E11) has been replaced with threonine (Fronticelli et al., 1993). The comparison of the structures of the natural and βV67T β-subunits reveals similar conformations even at the N-termini with the exception of the side chain of β2His. At the mutation site, only small changes in conformation of residues in the region of the distal heme pocket are observed confirming the structure prediction of the altered β-heme pocket. The mutant deoxyhemoglobin has no water molecule(s) present in either distal β-heme pocket in contrast to that observed for Thr[68](E11) myoglobin (Cameron et al., 1993). However, the increased polarity affects the functional characteristics of the distal heme pocket and its stability. The affinity for O_2, CO, and NO of the mutant subunits is decreased. The hemin dissociation rate is also decreased, while the rate of autoxidation is increased.

MATERIALS AND METHODS

Protein Cloning, Expression, and Purification. Complete details of the cloning of the β-globin gene and of the expression are described by Fronticelli and co-workers (1991). *Escherichia coli* cells were grown at 37 °C in an LB + ampicillin media to an OD_{600} of 0.600. Nalidixic acid was added (60 μg/mL), and the growth continued for 18 h. The cellular components were solubilized as described by Nagai and Thorgersen (1987), and the fusion protein was solubilized and reconstituted with α-globin and heme as described previously (Fronticelli et al., 1991). Human hemoglobin (HbA) was purified from outdated blood obtained from the Blood Bank of the University of Maryland (Bucci et al., 1988). Hemoglobin α-subunits were prepared as previously described (Bucci & Fronticelli, 1965). The recombinant βV67T was purified as previously described (Fronticelli et al., 1993).

Infrared Spectroscopy. HbA and βV67T were dialyzed against a CO-equilibrated, 100 mM phosphate buffer at pH 7.0. The hemoglobins were then removed from dialysis, and a 1:1 ratio of CO-equilibrated buffer containing sodium dithionite (2 mg/mL) was added to each sample in order to eliminate any residual methemoglobin.

A Perkin Elmer demountable sealed cell[2] equipped with CaF_2 windows and a 50 mm Teflon spacer was used for these experiments. The cell was flushed with CO just prior to the addition of the sample. The cell was then inserted into a Perkin Elmer 1600 Series FT-IR. Sample spectra were obtained using about 300 interferograms. The protein concentration was between 40 and 60 mg/mL.

Autoxidation. The autoxidation experiments were carried out in duplicate in a Hewlett Packard 8452A diode array spectrophotometer. Samples were prepared by adding 20 μL of a deoxygenated sodium dithionite solution (1 mg/mL) to 40 μL of 6% hemoglobin in order to remove any excess methemoglobin, and the resulting mixture was filtered on a Sephadex G25 column. The protein was concentrated to 40 mg/mL at 6 °C using a Millipore Ultrafree-HC filter, and 15 μL was added in a screw-cap spectrophotometric cuvette through a rubber serum stopper to 3 mL of buffer equilibrated with atmospheric concentrations of oxygen at 37 °C containing 100 mM sodium phosphate at pH 7.0, 1 mM EDTA, and catalase in a molar ration of 0.003 M catalase/heme. Absorption spectra were recorded for 48 h. The spectra were deconvolved between 400 and 700 nm using prerecorded standards of oxy-, met-, and deoxyhemoglobin, correcting for any base line drift. The resulting parameters derived from the spectral deconvolution were then normalized to relative percentages of oxy-, deoxy-, and methemoglobin in order to correct for any effects that might have occurred due to protein precipitation.

The disappearance of HbO_2 and the appearance of Hb(III) were simultaneously fitted using a nonlinear least-squares procedure (PSI-Plot, Polysoftware International) to the two multiphasic first-order rate equations (eqs 1 and 2):

$$[HbO_2] = \sum A_i \, x e^{-k_i t} \quad (1)$$

$$[Hb(III)] = \sum A_i \, x(1 - e^{-k_i t}) \quad (2)$$

where A_i is the amplitude of the ith phase, k_i is the rate constant of the ith phase, t is the time in minutes, and [HbO_2] and [Hb(III)] are the relative percentages of oxy- and methemoglobin. The spectra were recorded at room temperature (22 °C).

Heme Release. These measurements were done by Timothy L. Whitaker in the laboratory of Dr. John Olson using the methods and conditions described by Hargrove and co-workers (1994).

Rate of NO Release. Measurements of the rate of NO release were done according to the procedure described by Moore and Gibson (1976). Hemoglobin was degassed, under continuous stirring, in a spectrophotometric cuvette sealed with a serum stopper by flushing with humidified N_2 through

[1] Abbreviations: βV67T, mutant hemoglobin in which the β-chain Val[67](E11) has been replaced with Thr; HbA, purified human hemoglobin; HbAwt, recombinant wild type hemoglobin; 2HHB, the crystallographic structure of human deoxyhemoglobin determined by Fermi et al. (1984); PCR, polymerase chain reaction.

[2] Certain commercial equipment, instruments, and materials are identified in this paper in order to specify the experimental procedure. Such identification does not imply recommendation or endorsement by the National Institute of Standards and Technology nor does it imply that the material and equipment identified are necessarily the best available for the purpose.

Table 1: Crystallographic Parameters and Refinement Statistics for Deoxy-HbA and Deoxy-βV67T

	deoxy-HbA	deoxy-βV67T
space group	$P2_1$	$P2_1$
unit cell dimensions		
a (Å)	62.45	63.54
b (Å)	82.13	83.19
c (Å)	53.76	54.02
β (deg)	98.87	99.15
resolution (Å)	6.0−2.2	6.0−2.2
R_{sym}[a]	0.08	0.07
no. of reflections [$I > \sigma(I)$]	21 076	21 669
no. of protein atoms	4566	4566
no. of water molecules	474	434
R factor	0.137	0.149
deviations, rms:		
bond distances (Å)	0.016	0.017
angle distances (Å)	0.038	0.038

[a] $R_{sym} = \sum(I_{ij} - G_{ij}\langle I_j\rangle)/\sum|I_{ij}|$, where $G_{ij} = g_i + A_i s_j + B_i s_j^2$; $s = \sin\theta/\lambda$; and g, A, and B are scaling parameters.

two needles inserted into a serum stopper. To this solution, buffer equilibrated with NO was added to a 2-fold NO/heme molar excess. The reaction was started by adding a deoxygenated solution equilibrated with CO containing 7 mg of sodium dithionite/mL. For these conditions, due to the presence of a large excess of CO, the reaction is independent of heme and dithionite concentration. The reaction was followed at 442 nm. Measurements were performed at pH 9.3 in 0.1 M borate buffer. The rate of NO release was calculated using eq 1.

Molecular Modeling. Molecular modeling was carried out with Polygen QUANTA 2.1 and 2.3 Software (© York University, York, England) on a Silicon Graphics, Inc., IRIS-4D series workstation and with Insight II 2.3.0 San Diego: Biosym Technologies 1993 software on a Silicon Graphics, Inc., Iris Indigo XZ 4000 workstation. The molecular model of the distal heme pocket of the β-subunits of deoxy-βV67T was based on the human deoxyhemoglobin structure, 2HHB (Fermi et al., 1984). The molecular model of the distal heme pocket of the β-subunits of carbon monoxy-βV67T was based on the carbon monoxyhemoglobin structure, 1HCO (Baldwin, 1980), and porcine Thr^{68}(E11) carbon monoxymyoglobin structure, 1YCA (Cameron et al., 1993).

Protein Crystallization and X-ray Data Collection and Processing. The procedures for the crystallization of deoxy-HbA and deoxy-βV67T and X-ray data collection and processing are identical to that described by Fronticelli and co-workers (1994a). The crystallization of deoxy-HbA and deoxy-βV67T employed an adaptation of the procedure described by Perutz (1968). The XENGEN program system (Howard et al., 1987) was employed for X-ray data processing. The unit cell parameters and data processing statistics are summarized in Table 1.

Crystal Structure Determination and Refinement of Deoxy-HbA and Deoxy-βV67T. The starting model for the deoxy-HbA and deoxy-βV67T structures was the high-resolution deoxyhemoglobin structure (2HHB) determined by Fermi and co-workers (1984). Refinement was carried out using the X-PLOR 3.1 program package (Brunger, 1992). Initially, rigid-body refinement of first the tetramer followed by the individual subunits was applied to correct the position of the molecule in the unit cell. Using this procedure, the crystallographic R factors ($R = \sum|F_o - F_c|/\sum F_o$, summed over all hkl's) dropped significantly; for example, the initial value of 0.37 for the HbA structure dropped to 0.27. Next, simulated annealing was carried out with a slow cooling protocol (Brunger et al., 1990). The Engh and Huber (1991) geometric parameters for amino acid residues were used as the basis of the protein force field. The heme force field parameters used were developed by J. Kuriyan.[3] Empirical energy parameters for the water molecules were taken from TIP3p model of the program CHARMM. The full charges of Asp, Glu, Arg, and Lys were turned off during both dynamics and conventional minimization.

Prior to dynamics, the structures were minimized with 100 cycles of conjugant gradient minimization to relieve bad contacts. These minimized systems were heated to 4000 K by 5 ps dynamics using velocity scaling. They were then cooled to 300 K in 25 K temperature decrements every 50 steps. The time steps for molecular dynamics integration were set to 0.5 fs. Following dynamics, 150 cycles of conjugate gradient minimization were carried out to optimize the geometry and stereochemistry of the model. The final crystallographic R factors after annealing were 0.21 for deoxy-HbA and 0.22 for deoxy-βV67T.

Further refinement for both structures was carried out with conventional least-squares optimization of atomic coordinates and B factors (Hendrickson & Konnert, 1980; Hendrickson, 1985) with periodic adjustments of the model using FRODO (Jones, 1978) or O (Jones et al., 1991). Two types of electron density maps were used in the fitting, $2F_o - F_c$ and $F_o - F_c$ maps. Contour levels for the $2F_o - F_c$ and $F_o - F_c$ map ranged from 0.75σ to 1.0σ and from 2.0σ to 3.0σ, respectively. Multiple cycles of refinement followed by model adjustment were performed to eliminate difference peaks in the $F_o - F_c$ map above 3.0σ and account for all of the $2F_o - F_c$ electron density. A summary of the refinement statistics is presented in Table 1. The deoxy-HbA and deoxy-βV67T structures have been deposited in the Brookhaven Protein Data Bank (Bernstein et al., 1977) with entry identifiers 2HHD and 1HDB, respectively.

Protein Structure Comparison and Analysis. The comparisons of the crystallographic and modeled structures of hemoglobin were carried out by first using the program ALIGN (Satow et al., 1986) to superpose the structures. The structures were then visualized and distances between atoms measured using Quanta 2.1 and 2.3 (© York University, York, England), O (Jones et al., 1991), or FRODO (Jones, 1978). The comparison of the temperature factors resulting from the structure determinations of deoxy-HbA and deoxy-βV67T employed scaling the βV67T temperature factors relative to those of HbA.[4]

RESULTS

Structures of Human Deoxyhemoglobin and Deoxy-βV67T. The refinement of human deoxy-HbA with a virtually identical protocol to that of the mutant deoxy-βV67T was carried out to minimize differences between the structures of deoxy-βV67T and deoxy-HbA resulting from variations in experimental and/or refinement protocols. A preliminary report of the structure of deoxy-HbA was presented by Fronticelli and co-workers (1994a). The final structures of deoxy-HbA and deoxy-βV67T consist of the

[3] Unpublished data.

[4] Temperature factor scaling was carried out using the unpublished algorithm and programs of J. Dill and G. L. Gilliland.

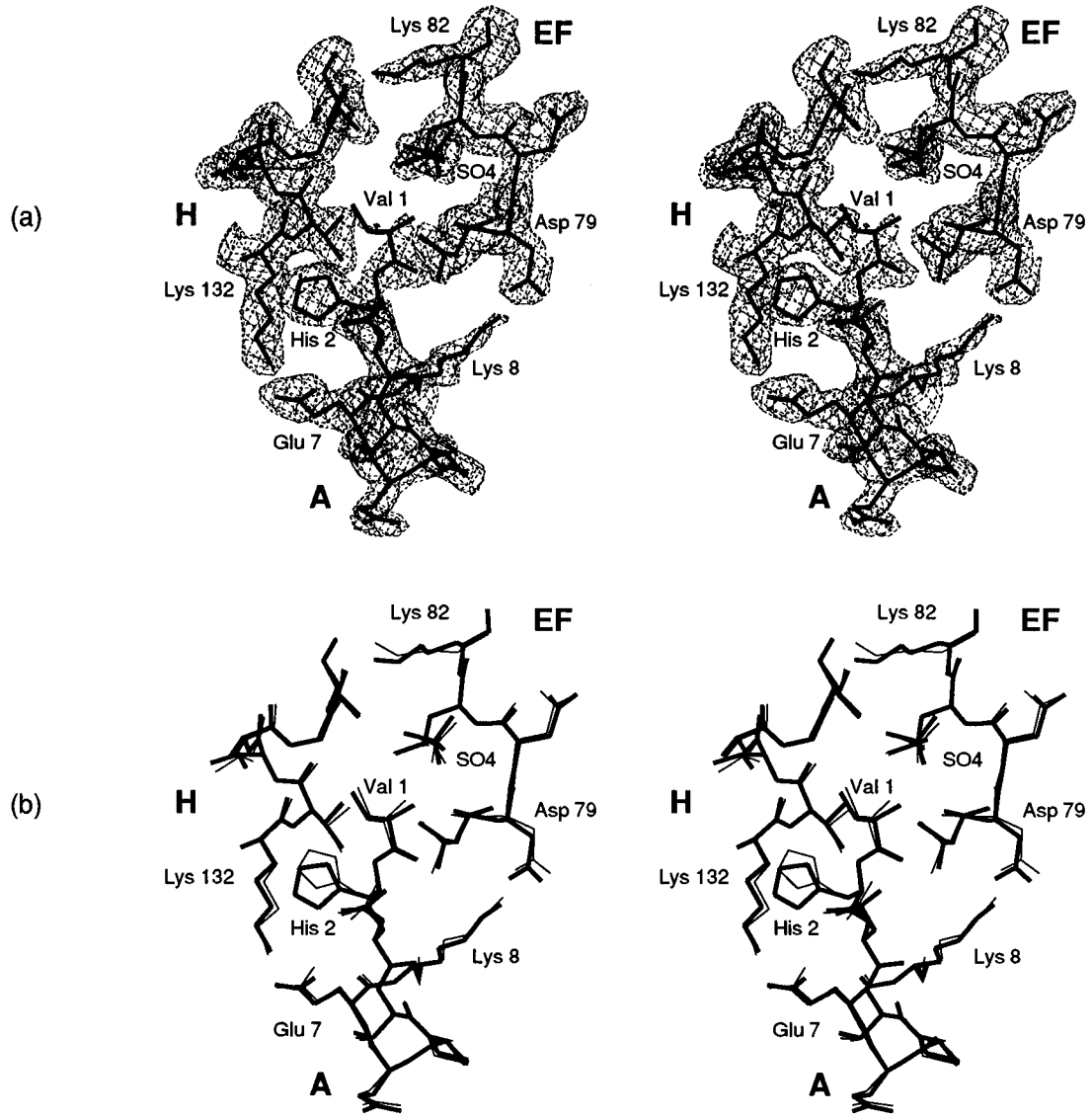

FIGURE 1: Stereoplots (a) of the final atomic model of the N-terminal region of the β_1-subunit of deoxy-βV67T superimposed on the $2F_o - F_c$ electron density map contoured at 1.0σ and (b) of the superposition of the N-terminal regions of β_1-subunits of deoxy-HbA and deoxy-βV67T. Bonds between atoms of deoxy-βV67T are indicated with thick lines, and those of the deoxy-HbA are indicated with thin lines. Specific regions of the molecule are indicated with large capital letters: **A**, **EF**, and **H**.

complete α- and β-globin polypeptides and the associated hemes along with 474 and 434 water molecules, respectively. A sulfate ion is found associated with each of the β-subunits of both the deoxy-HbA and deoxy-βV67T as seen in the HbA structure (Fermi et al., 1984). The structures of deoxy-HbA and deoxy-βV67T have crystallographic *R* values of 0.137 and 0.149, respectively. A portion of the final electron density map in the vicinity of the β_1-subunit N-terminus is illustrated in Figure 1a. The final structure of the deoxy-HbA and the starting model (Fermi et al., 1984) are very similar (0.4 Å rms for all C$^\alpha$'s when the complete tetramers are compared) except that the two differ in their representations of the sulfate ions, the number of water molecules and the conformations of a number of side chains, especially those that are positively or negatively charged.

The similarity of the structures of deoxy-βV67T and deoxy-HbA is revealed in the results of a direct comparison (Table 2). There is an overall rms difference of 0.38 Å between positions of C$^\alpha$'s of the two structures and even better agreement when the dimers and monomers of the protein are compared (Table 2) with the α-subunits of the two structures having the best agreement. A temperature factor analysis of both structures including both averaging for the assembly units of the tetramer (Table 3) and temperature factor profiles (Figure 2) for β_1-subunits of the deoxy-HbA and the deoxy-βV67T also illustrates the congruity of the natural and recombinant structures.

Table 2: Root Mean Square Differences (Å) Between the Aligned Structures of Deoxy-HbA and Deoxy-βV67T

globin subunits	C$^\alpha$ pairs	rms (Å)
$\alpha_1\alpha_2\beta_1\beta_2$	570	0.38
$\alpha_1\beta_1$	285	0.28
$\alpha_2\beta_2$	285	0.28
α_1	140	0.24
β_1	145	0.25
α_2	140	0.24
β_2	145	0.26

The recombinant β-globin is expressed as part of a fusion protein that undergoes proteolytic cleavage with factor Xa producing a β-globin polypeptide that is then combined with the heme and the native α-subunits to produce tetrameric hemoglobin (Fronticelli et al., 1993). A least-squares superposition of the N-terminal regions of β-subunits of the

Table 3: Average Temperature Factors, $\langle B \rangle$ (Å^2), for All Atoms of Deoxy-HbA and Deoxy-βV67T

	deoxy-HbA	deoxy-βV67T
$\alpha_1\alpha_2\beta_1\beta_2$	15.2	15.2 (20.7)[a]
$\alpha_1\beta_1$	15.5	15.8 (21.4)
$\alpha_2\beta_2$	14.8	14.6 (20.1)
α_1	15.3	14.8 (20.3)
β_1	15.6	16.8 (22.3)
α_2	13.5	13.4 (18.9)
β_2	16.0	15.7 (21.2)

[a] Values in parentheses indicate the value of the temperature factors from the crystallographic refinement prior to scaling using the procedure described in the Materials and Methods section.

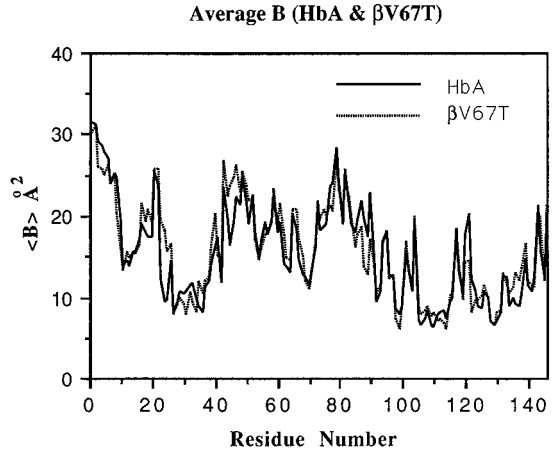

FIGURE 2: Plots of sequence number vs temperature factors, $\langle B \rangle$ (Å^2) for β_1-subunit of deoxy-HbA (solid line) and β_1-subunit of deoxy-V67T (dotted line).

deoxy-HbA and the deoxy-βV67T indicates the similarity in the conformations of this region. However, there is an appreciable difference in the conformation of the β2His side chains as shown Figure 1b. The temperature factor profiles of the N-terminal region of the β-chains (Figure 2 for the β_1-subunits) also reflects the structural homology of this region of the proteins.

The comparison of the specific interactions of the N-terminal regions of the deoxy-HbA and the deoxy-βV67T β-subunits (Figure 1) further illustrates the similarities between the structures. A sulfate ion is present near the N-terminus of both structures. This anion has also been observed in the 2HHB structure (Fermi et al., 1984) and in two N-terminal mutant structures determined by Kavanaugh and co-workers (1992). In deoxy-HbA the sulfate ion forms a complex network of hydrogen bonds and electrostatic interactions. A preliminary description of the interactions was recently reported by Fronticelli and co-workers (1994a). Atom O1 of the sulfate ion is located between N-terminal N atom (3.5 Å) and N$^\zeta$ atom (5.0 Å) of β_1Lys^{82}. A distance of 2.9 Å is also observed between atom O1 of the sulfate and a water molecule. Sulfate ion atom O2 interacts only with the N-terminal N atom (3.1 Å) of β_1Val^1. The O3 atom of the sulfate ion forms a hydrogen bond with the N atom (3.5 Å) of β_1Lys^{82}. The O4 atom also interacts with the N-terminal N atom (2.6 Å) of β_1Val^1 and also forms a strong hydrogen bond (2.0 Å) with the N atom of β_1Leu^{81}. A sulfate ion and similar interactions are observed at the N-terminus of the β_2-chain. Thus, the sulfate ions are anchored to the β-chains by complex networks of hydrogen bonds and electrostatic interactions with the EF corners and the N-termini.

The N atom of β_1Val^1, in addition to interacting with the three oxygen atoms of the sulfate ion, also is a hydrogen donor in a hydrogen bond with the O atom of β_1Leu^{78}. The side chain of β_1Val^1 is buried in a hydrophobic pocket composed of side chains from β_1Leu^3, β_1Leu^{78}, β_1Leu ^{81}, β_1Val^{133}, and β_1Gly^{136}. Nearby, the side chains of β_1Lys^8 and β_1Asp^{79} form another important electrostatic interaction in this region. The atoms O$^{\delta 1}$ and O$^{\delta 2}$ are both 3.5 Å from the N$^\zeta$ atom of β_1Lys^8.

Distal Heme Pocket of Deoxy-βV67T. The electron density map of deoxy-βV67T for both of the distal heme pockets of the β-subunits was unambiguous. The temperature factors for atoms of residues associated with the heme pocket were below the average value for all atoms (15.2 Å^2), indicating that the atomic positions at this site are well defined. The $2F_o - F_c$ electron density map for the heme and residues associated with distal heme pocket are shown in Figure 3a.

The isosteric substitution of threonine for Val^{67}(E11) in the distal heme pocket produces nearly imperceptible changes in protein conformation compared to that observed for deoxy-HbA (see Table 2). The changes that are present are local to the site of mutation (Figure 3b). There is no significant change in the positions of the backbone atoms of the E helix, nor is there any significant change in the side chain rotamer only slight perturbations in the ϕ and ψ angles of this residue (Table 4). The side chain position of the distal histidine, His^{63}(E7), is rigidly maintained, and there is no perceptible alteration in the orientation of the heme. The O$^\gamma$ atom of the β_1Thr^{67}(E11) is positioned to act as a hydrogen donor in the formation of a hydrogen bond with the backbone carbonyl oxygen atom of His^{63}(E7). The distance between these two atoms is 2.9 Å. The O$^\gamma$ atom is within 3.5 and 3.9 Å of the His^{63}(E7) side chain nitrogens, N$^\delta$ and N$^\epsilon$, respectively, but the geometry is not suitable, in either case, to produce a strong hydrogen bond. The oxygen atom of the threonine side chain, at 4.7 Å, is too far to directly interact with the Fe atom of the heme.

The β_2-subunit Thr^{67}(E11) is positioned in nearly the same orientation (Table 4) as observed for the β_1-subunit. The O$^\gamma$ atom of Thr^{67}(E11) which is 2.8 Å from the carbonyl oxygen of His^{63} (E7) participates as a proton donor in a hydrogen bond. The O$^\gamma$ atom is also quite distant from the His^{63}(E7) nitrogens, N$^\delta$ and N$^\epsilon$, at 4.4 and 3.7 Å, respectively. The distance to the Fe atom is also nearly the same, 4.8 Å. Thus, the environments of the two β-subunit distal heme pockets are virtually identical.

The crystal structure of the recombinant porcine Thr^{68}(E11) myoglobin has recently been determined (Cameron et al., 1993). The crystallographic asymmetric unit in this structure determination contains two independent monomers of Thr^{68}(E11) deoxymyoglobin, labeled A and B in the coordinate data set. The environment of the distal heme pockets of β-subunits of HbA and of the porcine myoglobin are very similar in the vicinity of the E11 residue except for the substitution of a threonine for a lysine at residue E10 in the porcine myoglobin. The Ell residues of both of the Thr^{68}(E11) deoxymyoglobin monomers in the asymmetric unit have virtually identical side chain conformations as those found in the β-subunits of βV67T (Table 4), but the local environment of this residue includes the presence of two

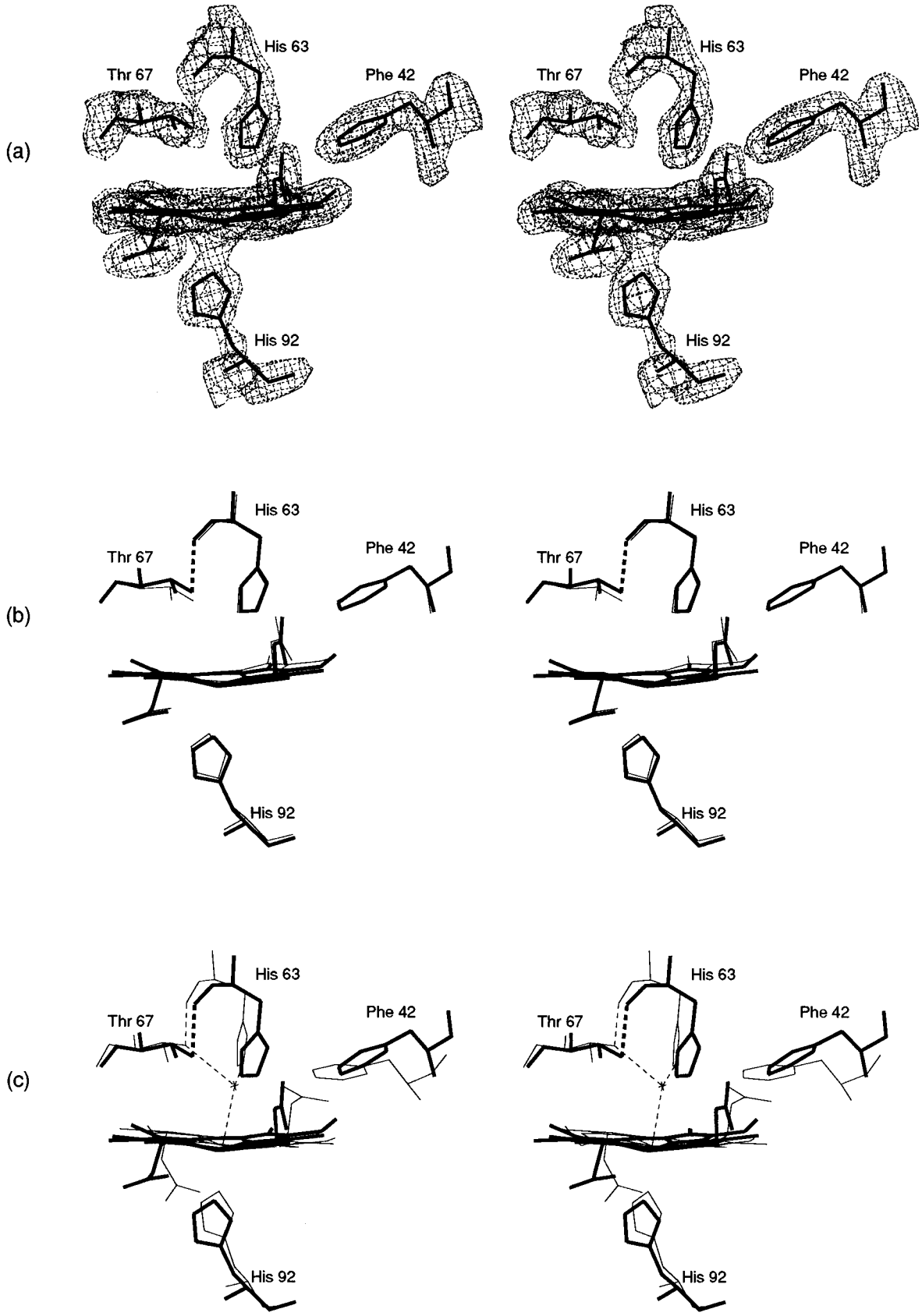

FIGURE 3: Stereoplots (a) of the atomic model of the distal heme pocket of the β_1-subunit of deoxy-βV67T superimposed on the $2F_o - F_c$ electron density map contoured at 1.0σ and (b) of the superposition of the distal heme pockets of the β_1-subunits of deoxy-HbA and deoxy-βV67T. Bonds between atoms of deoxy-βV67T are indicated with thick lines, those of the deoxy-HbA are indicated with thin lines, and possible hydrogen bonds are represented with dashed lines. (c) Stereoplot of the atomic model of the distal heme pocket of the β_1-subunit of deoxy-βV67T superimposed on that of the deoxymyoglobin monomer B. Bonds between atoms of deoxy-βV67T are indicated with thick lines, those of the deoxymyoglobin monomer B are indicated with thin lines with an asterisk denoting the position of the distal heme pocket water, and possible hydrogen bonds are represented with dashed lines.

Table 4: Torsion Angles (deg) for Thr/Val(E11) and His(E7) for Hemoglobin A, and Mutant Hemoglobin, and Myoglobina

	Thr/Val (E11)			His (E7)			
	ϕ	Ψ	χ_1	ϕ	Ψ	χ_1	χ_2
HbA (β_1)	−60	−58	172	−67	−34	−169	54
HbA (β_2)	−50	−57	159	−66	−45	−168	69
βV67T (β_1)	−63	−28	−171[b]	−68	−44	−168	53
βV67T (β_2)	−64	−28	178[b]	−63	−48	−163	56
V68T Mb_A	−65	−50	176[b]	−60	−35	−165	61
V68T Mb_B	−65	−49	179[b]	−70	−35	−169	71

[a] V68T Mb_A and V68T Mb_B represent independent monomers A and B in the myoglobin crystal lattice, respectively. [b] χ_1 torsion angle calculated equating Val $C^{\gamma 1}$ and $C^{\gamma 2}$ to Thr $C^{\gamma 2}$ and $O^{\gamma 1}$, respectively.

water molecules and one water molecule for Thr[68](E11) deoxymyoglobin monomer A and B, respectively. No water is present in the distal heme pockets of either of the two β-subunits of βV67T. A superposition of the distal heme pocket of the Thr[68](E11) deoxymyoglobin monomer B containing a single water molecule onto that of βV67T is shown in Figure 3c. The agreement of the positions of the side chains is quite good considering the differences in the amino acid sequences of these two globin chains. The position of the proximal histidine with respect to the iron atoms for both molecules is within experimental error of the coordinates.

Molecular Modeling of Deoxy- and Carbon Monoxy-βV67T. Molecular modeling studies were carried out prior to the crystallographic studies to examine possible modification of the heme pocket resulting from the substitution of the valine with threonine at position E11. The likelihood of interaction between the βThr[67](E11) and βHis[63](E7) was considered. A possible conformation of the E11 side chain places the hydroxyl of the threonine approximately 3.0 Å from the backbone carbonyl oxygen at residue E7 (i.e., at $n - 4$), allowing formation of a hydrogen bond. A hydrogen bond between a side chain at position (n) and the peptide carbonyl oxygen of the residue at ($n - 4$) is the most commonly observed side chain-to-backbone hydrogen bond involving a backbone carbonyl group (Baker & Hubbard, 1984), and it is typically found in regions of helical conformation of the main chain.

In the modeled deoxy-βV67T, interactions of the threonine hydroxyl group with either βHis[63](E7) N^{δ} or N^{ϵ} acting as an acceptor are possible, creating an alternative of a bifurcated hydrogen bond. Without a major shift at the position of the E7 side chain, the geometry of these interactions is very poor. On the other hand, a double hydrogen bond arrangement with a protonated N^{δ} as a donor and the threonine hydroxyl oxygen as an acceptor in addition to the hydroxyl-to-backbone hydrogen bond seems rather unlikely. In the final modeled deoxy-βV67T structure, the Thr[67](E11) side chain has therefore been adjusted to conform with the geometry of a hydrogen bond between its hydroxyl group and the backbone carbonyl of His[63](E7).

No water was included in the distal heme pocket of the modeled structure although a water molecule has been found in that of the porcine Thr[68](E11) deoxymyoglobin mutant (Smerdon et al., 1991). There is no water molecule in the distal heme pocket of the human hemoglobin while it has been identified in the wild type deoxymyoglobin structures[5] (Quillin et al., 1993). In both the mutant and wild type myoglobins positions of the side chains of residues E11 (Val or Thr) and E7 (His) relative to the β-heme group are different than in human deoxyhemoglobin (Fermi et al., 1984), enough to significantly affect the energetics and ordering of a water moleule. The vector that describes this relative shift (for both side chains) is approximately parallel to the plane of the heme, perpendicular to the line joining the two side chains, and about 1 Å in magnitude. Therefore, extrapolating from the case of deoxymyoglobin to deoxyhemoglobin requires caution.

The structure of the model of the βThr[67](E11) agrees quite well with the crystallographic structure. The positions of βThr[67](E11) for both structures are similar; the slight discrepancy in the structures can be accounted for by a rotation of χ_1 by +31 or +24° for β_1 and β_2, respectively. The differences between the observed and modeled β_1 subunit residues are visible in the structure comparison illustrated in Figure 4a.

In the modeled carbon monoxy-βV67T the Thr[67](E11) side chain has also been adjusted to conform with the geometry of a hydrogen bond between its hydroxyl group and the backbone carbonyl of His[63](E7). A formation of a hydrogen bond with the peptide backbone would place the partial-negative charge of the hydroxyl oxygen of the threonine near the ligand as already observed in the case of Thr[68](E11) myoglobin (Cameron et al., 1993). A comparison of the modeled structure of carbon monoxy-βV67T with the porcine carbon monoxymyoglobin monomer A is illustrated in Figure 4b.

Infrared Spectroscopy. Infrared spectra of the carboxy derivatives of HbA, recombinant wild type hemoglobin (HbAwt) and βV67T are illustrated in Figure 5. HbA and HbAwt both show a single peak with a maximum at 1950 cm^{-1} that contains the overlapping contribution from the carboxy derivative of α- and β-subunits (Potter et al., 1990). The additional small components reported by Potter et al. (1990) (<5%) are not in high enough amounts to be resolved by our analysis. This absorption was assigned to the stretching frequency of CO (Alben & Caughy, 1968) and indicates that the CO stretch of the α- and β-subunits occurs at the same frequency. In the infrared spectrum of carbon monoxy-βV67T, two peaks are detected, one at the same wavelength observed for HbA and a second that is shifted toward a higher frequency with a maximum at 1968 cm^{-1}, probably contributed by the mutated β subunits. A similar shift toward a higher frequency was observed in the analogous distal heme pocket mutant of porcine myoglobin (Cameron et al., 1993).

Autoxidation. The time courses for the autoxidation of natural HbA, HbAwt, and βV67T are shown in Figure 6, and the full lines represent the calculated fit to the experimental data. For natural HbA, the experimental points could be described by a single-exponential expression. For wtHbA and βV67T experimental points were fitted to a first-order biphasic rate equation for which the first points contain 10% and 30% methemoglobin, respectively. The recovered rate constants are reported in Table 5.

[5] Unpublished structure of deoxymyoglobin that was deposited in the Brookhaven Protein Data Bank as entry 1MBD by S. E. V. Philips in 1981.

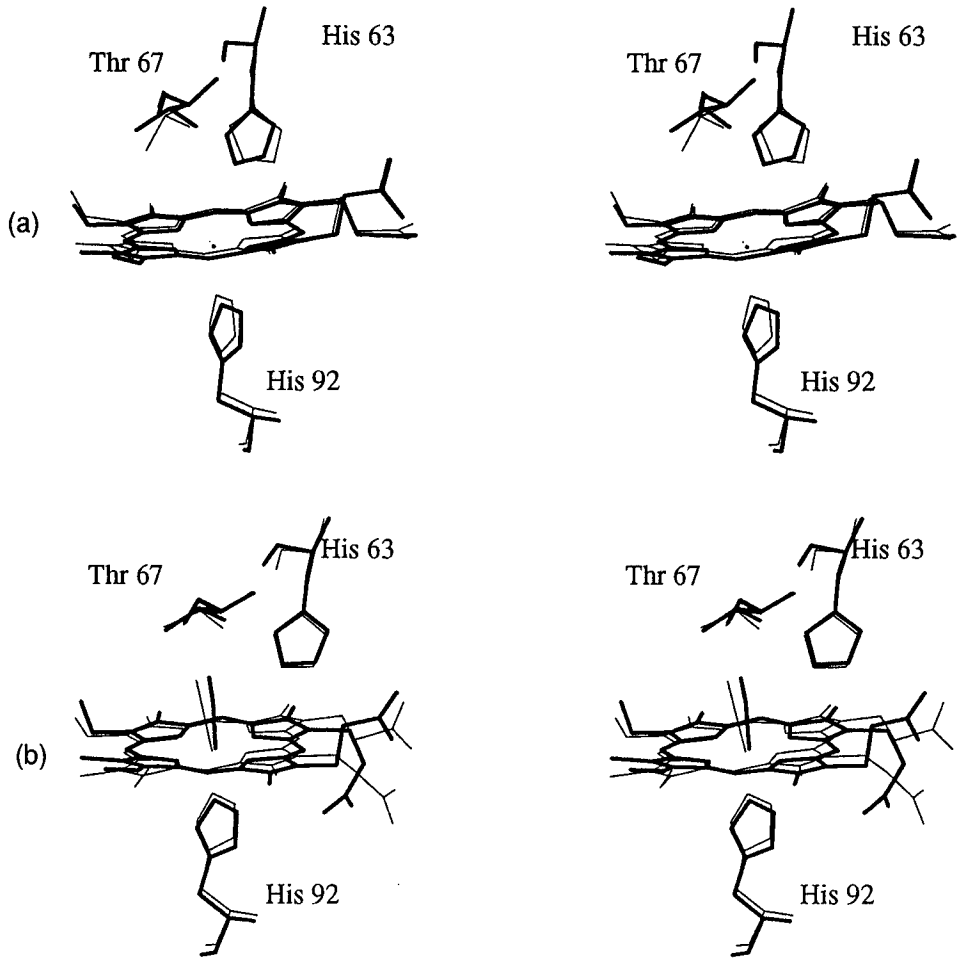

FIGURE 4: Stereoplots of the heme, Thr[67](E11), His[63](E7), and His[92](F8) of (a) the crystallographic structure of deoxy-βV67T with thick lines and the modeled structure of deoxy-βV67T with thin lines and (b) of the crystallographic structure of carbon monoxymyoglobin monomer A (1YCA) with thick lines and the modeled structure of carbon monoxy-βV67T with thin lines.

In βV67T the calculated oxidation rates differ 34-fold. In HbAwt, the two rates differ 10-fold and the fast phase is 25% of the total. The rate of the slow phase of wtHbA is similar to natural HbA, but in βV67T it remains 2.6-fold faster.

Heme Transfer. The heme transfer rates of the aquomet derivatives of the α- and β-subunits of variant hemoglobin, βV67T, have been compared with those of natural HbA using the hemin dissociation method described by Hargrove and co-workers (1994). It is well recognized that hemin dissociates more readily from the β-subunits than from the α-subunits of hemoglobin (Bunn & Jandl, 1968), giving rise to a reaction time course that can be fitted with the sum of two exponential terms. The rates of hemin dissociation are nearly the same for the α-subunits of both natural HbA and βV67T, 0.5 and 0.6 h^{-1}, respectively. In contrast, the rate of heme release was 6-fold slower for the β-subunit of βV67T from that found for natural HbA. The values for the hemin dissociation constants are 2 and 12 h^{-1} between 6 and 10 μM heme concentration for β-subunit of βV67T and HbA, respectively.

Nitric Oxide Dissociation. The rate of NO dissociation was measured in the nitrosyl derivatives of HbA and βV67T. In the HbA the replacement is described by a single exponential, and the calculated NO dissociation constant is 0.027 h^{-1}. The observed time course of βV67T is biphasic and is described by two exponentials of equal fractional amplitude. The slower rate is similar to that of HbA, and the faster is 1 order of magnitude larger. The calculated NO dissociation constants are 0.191 and 0.020 h^{-1} for the fast and slow phases, respectively.

DISCUSSION

N-Termini Processing, Folding, and Assembly. The expression system used for these studies (Fronticelli et al., 1991) is a modification of the original system developed by Nagai and Thogersen (1984). With this construct, the β-globin is cleaved precisely before the N-terminal valine and has the N-terminal sequence of the natural β-globin. The mutant hemoglobin obtained contains natural α-subunits, thus, modifications in the functional and/or conformational properties can be assigned to the recombinant β-subunits.

The electron density map of the β-subunit chains of βV67T confirms that the variant N-termini are nearly identical to that observed for natural hemoglobin. The comparison of the structures of HbA and βV67T in this region indicates nearly identical backbone and side chain conformations, location of solvent and sulfate, hydrogen bonds, and electrostatic interactions (Figure 1b). In addition, the temperature factor (*B*) profiles of the β-subunits of both HbA and βV67T are also in good agreement (see Table 3 and Figure 2).

Influence of the Presence of the Thr[67](E11) on the Structure of the Distal Heme Pocket of Deoxy-β-subunit. The replacement of valine with threonine in the distal-heme binding pocket induces only subtle changes in the local

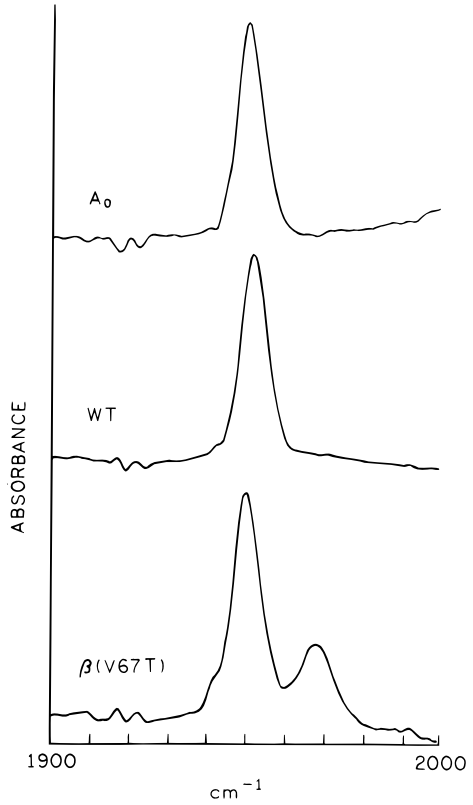

FIGURE 5: FTIR spectra of carbon monoxy samples of HbA, wtHbA, and βV67T. All spectra have been corrected for the buffer background.

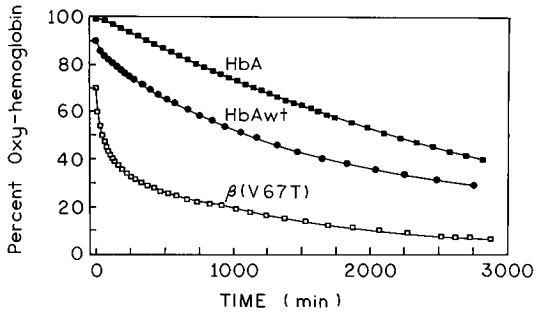

FIGURE 6: Time course of the oxidation of HbA, wtHbA, and βV67T.

geometry even though the polarity changes significantly. The X-ray crystallographic structure confirms the modeling results. In particular, a hydrogen bond is observed between the O^{γ} atom of Thr^{67}(E11) and the backbone carbonyl of His^{63}(E7).

There is an absence of electron density for a water molecule in the distal heme pocket in the deoxy structure of βV67T even though the volume of the cavity in the distal heme pocket would accommodate a water molecule, and an examination of the access to the distal heme pocket would not preclude water's entry. The absence of electron density reflects either that there is no water present or that a water molecule is present but is disordered. In contrast, the structure of deoxymyoglobin, with two molecules in the asymmetric unit, has a water molecule(s) associated with each of the independent sites. There has also been a recent structural report of Hb Chico, a hemoglobin variant in which βLys^{66}(E10) is replaced with a threonine (Bonaventura et al., 1991). This is a residue adjacent to Val^{67}(E11) and is close to the distal histidine. This change introduces a difference in polarity of the heme pocket lowering the oxygen affinity in a manner similar to that observed for βV67T. A difference Fourier study of crystals of the deoxy form of this variant indicates a water bridging the Thr^{66}(E10) and His^{63}(E7) residues. In a previous paper we reported the equilibrium of O_2 binding and the kinetics of O_2 and CO binding to βV67T (Fronticelli et al., 1993). Here we present further functional characterization of this mutant with regard to its increased susceptibility to autoxidation, interaction with CO and NO, and stability of the heme complex.

Table 5: Autoxidation Rates for Natural Human Hemoglobin (HbA), Recombinant Human Hemoglobin (HbAwt), and βV67T[a]

hemoglobins	A[b]	k (min^{-1})
HbA	1.00	0.000 316 (3)
HbAwt	0.18 (3)	0.003 03 (5)
	0.71 (4)	0.000 33 (4)
βV67T	0.26 (2)	0.028 1 (6)
	0.45 (3)	0.000 82 (3)

[a] The measurements were done at 37 °C in 100 mM phosphate buffer, 1 mM EDTA at pH 7.0. Catalase was added in the sample in a molar ratio of 0.0003/heme. The numbers in parentheses represent the standard error for each experiment. [b] A is the relative fraction of each kinetic phase.

Infrared Spectroscopy. No modifications are observed in the IR spectra of carbon monoxy derivatives of HbA and HbAwt which are consistent with the observations of Potter et al. (1990), and the spectra show one dominant component representing the contribution from the α- and β-subunits. Both HbA and HbAwt spectra are very similar, indicating equal contributions of native and recombinant β-subunits to the C−O stretch shown in the IR spectrum. In contrast, the IR spectrum of carbon monoxy-βV67T shows the presence of a second band at 1968 cm^{-1}. A similar IR band has been observed ion other natural mutant hemoglobins with increased heme pocket polarity; however, it is of smaller intensity (Potter et al., 1990).

In pig myoglobin this same mutation (V68T) produces a quantitatively similar increase in ν_{CO} (Cameron et al., 1993). The modified frequency observed in βV67T is not due to stereochemical modification of the heme pocket, as shown by the crystallographic analysis. The intensity of the peak at 1968 cm^{-1} is smaller than that at 1950 cm^{-1}. This suggests that the βV67T has probably some of its absorbance intensity in the 1950 cm^{-1} region. It may indicate the presence of multiple CO orientational conformers in the mutant β-subunits.

The modified IR spectrum observed for βV67T is consistent with the proposition of others (Cameron et al., 1993; Balasubramanian et al., 1993; Li et al., 1994) that the CO stretching frequency is governed largely by electrostatic interactions in the heme pocket. A significant interaction between β67Thr side chain and coordinated CO is also evident by a difference in the temperature dependence of the Soret absorbance of carboxy βV67T compared to that of carboxy HbAwt (Militello et al., 1995).

Autoxidation. In natural HbA, the rate of autoxidation is similar for the α- and β-subunits; for HbAwt the reaction was biphasic, with a phase 10-fold faster than natural HbA. The proteins used for these experiments were highly purified, so it is unlikely that this is due to the presence of contaminants. Also, the functional properties (Fronticelli et al., 1991) and the dimer−tetramer association constants

(Fronticelli et al., 1994b) of the HbAwt are very similar to those of natural HbA. CD (Fronticelli et al., 1991; Yanase et al., 1994) and NMR spectra (Shen et al., 1993), however, suggest the presence of some heme disorder in the recombinant β-subunits. It can be hypothesized that in HbAwt, heme disorder is associated with a faster autoxidation rate. In βV67T the rate of the fast phase is increased 90-fold with respect to HbA. The fast phase can be attributed to the mutant β-subunits, and the slow phase can be attributed to the natural α-subunits. A possibility is that the increased polarity of the heme pocket favors the dissociation of oxygen in the superoxide form. Although the exact mechanism of methemoglobin formation still remains unclear, superoxide dissociation has been postulated as a major pathway for methemoglobin formation (Brantley et al., 1993).

Heme Transfer. A decrease in the rate of hemin release was measured in porcine and sperm whale mutant myoglobins with a threonine at position E11 (Hargrove et al., 1994). This has been attributed to the presence of a hydrogen bond between the coordinated water molecule and the O^{γ} of the threonine. In the ferric form used for the heme transfer experiments a water molecule is coordinated to the heme also in the β-subunit chains, and the same interpretation applies.

Nitric Oxide Dissociation. In human hemoglobin the rate of NO release is the same for the α- and β-subunits. In βV67T the rate becomes biphasic. The slow rate is similar to that of HbA and can be assigned to the α-subunits; the fast rate is increased by 1 order of magnitude and can be assigned to the mutant β-subunits. The off rates of both CO (Fronticelli et al., 1993) and NO are increased. Since these are both diatomic ligands, their interaction with the threonine side chain would be expected to be qualitatively similar.

Conclusions. The three-dimensional structure of the deoxy-βV67T reveals that there is little effect on the structure of the distal heme pocket by the isosteric substitution of threonine for valine. Unlike the deoxy structures of Hb Chico, βK66T(E10) (Bonaventura et al., 1991), and porcine myoglobin, V68T(E11) (Cameron et al., 1993), a water molecule is not present in the distal heme pocket of βV67T. The O^{γ} of βThr^{67} is involved in a hydrogen bond with the backbone O of βHis^{64}, and the polar hydroxyl group's presence in the distal heme pocket modifies the interaction of the Fe with ligands. In the carbon monoxy and nitrosyl derivatives a dipolar interaction with the O^{γ} of β67Thr is possibly established. The increased polarity of the heme pocket decreases the affinity for oxygen, increasing the rate of methemoglobin formation. In the aquomet derivative the water molecule that has been shown to coordinate with Fe(III) (Ladner et al., 1977) probably hydrogen bonds with the threonine O^{γ}, providing additional stabilization to the hemin−protein complex.

ACKNOWLEDGMENT

We are grateful to Walter Kisiel, Department of Pathology, University of New Mexico, for the gift of factor Xa. We also thank John Olson and Timothy Whitaker for the use of the hemin transfer data.

REFERENCES

Alben, J. O., & Caughey, W. S. (1968) *Biochemistry* 7, 175−181.
Baker, E. N., & Hubbard, R. E. (1984) *Prog. Biophys. Mol. Biol. 44*, 97−179.
Balasubramanian, S., Lambright, D. G., & Boxer, S. G. (1993) *Proc. Natl. Acad. Sci. U.S.A. 90*, 4718−4722.
Baldwin, J. M. (1980) *J. Mol Biol. 136*, 103−128.
Bernstein, F. C., Koetzle, T. F., Williams, G. J. B., Meyer, E. F., Jr., Brice, M. D., Rogers, J. R., Kennard, O., Shimanouchi, T., & Tasumi, M. (1977) *J. Mol. Biol. 112*, 535−542.
Bonaventura, C., Cashon, R., Bonaventura, J., Perutz, M., Fermi, G., & Shih, D. T.-B. (1991) *J. Biol. Chem. 266*, 23033−23040.
Brunger, A. T. (1992) *X-PLOR, Version 3.1*, Yale University Press, New Haven, CT.
Brunger, A. T., Krukowski, A., & Erickson, J. (1990) *Acta Crytallogr. A46*, 585−593.
Brantley, R. E., Jr., Smerdon, S. J., Wilkinson, A. J., Singleton, E. W., & Olson, J. S. (1993) *J. Biol. Chem. 268*, 6995−7010.
Bucci, E., & Fronticelli, C. (1965) *J. Biol. Chem. 240*, PC551.
Bucci, E., Malak, H., Fronticelli, C., Gryczynski, I., Laczko, G., & Lakowicz, J. R. (1988) *Biophy. Chem. 32*, 187−198.
Bunn, H. F., & Jandl, J. H. (1968) *J. Biol. Chem. 243*, 465−475.
Cameron, A. D., Smerdon, S. J., Wilkinson, A. J., Habash, J., Helliwell, J., Li, T., & Olson, J. S. (1993) *Biochemistry 32*, 13061−13070.
Carver, T. E., Rohlfs, R. J., Olson, J. S., Bigson, Q. H., Blackmore, R. S., Springer, B. A., & Sligar, S. G. (1990) *J. Biol. Chem. 265*, 20007−20020.
Carver, T. E., Olson, J. E., Smerdon, S. J., Krzywda, S., Wilkinson, A. J., Gibson, Q. H., Blackmore, R. S., Ropp, J. D., & Sligar, S. G. (1991) *Biochemistry 30*, 4697−4705.
Carver, T. E., Brantley, R. E., Jr., Singleton, E. W., Arduini, R. M., Quillin, M. L., Phillips, G. N., Jr., & Olson, J. S. (1992) *J. Biol. Chem. 267*, 14443−14450.
Egeberg, K. D., Springer, B. A., Sligar, S. G., Carver, T. E., Rohlfs, R. J., & Olson, J. S. (1990) *J. Biol. Chem. 265*, 11788−11795.
Engh, R. A., & Huber, R. (1991) *Acta Crystallogr. A47*, 392−400.
Fermi, G., Perutz, M. F., Shaanan, B., & Fourme, R. (1984) *J. Mol. Biol. 175*, 159−174.
Fronticelli, C., O'Donnell, K., & Brinigar, W. S. (1991) *J. Protein Chem. 10*, 495−501.
Fronticelli, C., Brinigar, W. S., Olson, J. S., Bucci, E., Gryczynski, Z., O'Donnell, J. K., & Kowalczyk, J. (1993) *Biochemistry 32*, 1235−1242.
Fronticelli, C., Pechik, I., Brinigar, W. S., Kowalczyk, J., & Gilliland, G. L. (1994a) *J. Biol. Chem. 269*, 23965−23969.
Fronticelli, C., Gattoni, G. M., Lu, A.-L., Brinigar, W. S., Bucci, J. L., & Chiancone, E. (1994b) *Biophys. Chem. 51*, 53−57.
Hargrove, M. S., Krzywda, S., Wilkinson, A. J., Dou, Y., Masso, I.-S., & Olson, J. S. (1994) *Biochemistry 33*, 11767−11775.
Hendrickson, W. (1985) *Methods Enzymol. 115*, 252−270.
Hendrickson, W., & Konnert, J. (1980) in *Computing in Crystallography* (Diamond, R., Ramaseshan, S., & Venkatesan, K., Eds.) pp 1301−1323, Indian Academy of Sciences, Bangalore, India.
Howard, A. J., Gilliland, G. L., Finzel, B. C., Poulos, T. L., Ohlendorf, D. H., & Salemme, F. R. (1987) *J. Appl. Crystallogr. 20*, 383−387.
Jones, T. A. (1978) *J. Appl. Crystallogr. 11*, 268−272.
Jones, T. A., Zou, J.-Y., Cowan, S. W., & Kjeldgaard, M. (1991) *J. Appl. Crystallogr. 11*, 268−272.
Li, X.-Y., & Spiro, T. G. (1988) *J. Am. Chem. Soc. 110*, 6024−6033.
Kavanaugh, J. S., Rogers, P. H., & Arnone, A. (1992) *Biochemistry 31*, 8640−8647.
Ladner, R. C., Heidner, E. J., & Pertuz, M. F. (1977) *J. Mol. Biol. 114*, 385−415.
Li, T., Quillin, M. L., Phillips, G. N., & Olson, J. S. (1994) *Biochemistry 33*, 1433−1446.
Mathews, A. J., Rohlfs, R. J., Olson, J. S., Tame, J., Renaud, J.-P., & Nagai, K. (1989) *J. Biol. Chem. 264*, 16573−16583.
Militello, V., Cupane, A., Leone, M., Brinigar, W. S., Lu, A.-L., & Fronticelli, C. (1995) *Proteins: Struct. Funct. Genet. 22*, 12−19.
Nagai, K., & Thogersen, H. C. (1984) *Nature 309*, 810−812.
Nagai, K., & Thogersen, H. C. (1987) *Methods Enzymol. 153*, 461−481.

Nagai, K., Perutz, M. F., & Poyart, C. (1985) *Proc. Natl. Acad. Sci. U.S.A. 82*, 7252−71255.

Nagai, K., Luisi, B., Shih, D., Miyazaki, G., Imai, K., Poyart, C., De Young, A., Kwiatkowsky, L., Noble, R. W., Lin, S.-H., & Yu, N.-T. (1987) *Nature 329*, 858−860.

Olson, J. S., Mathews, A. J., Rohlfs, R. J., Springer, B. A., Egeberg, K. D., Sligar, S. G., Tame, J., Renaud, J.-P., & Nagai, K. (1988) *Nature 366*, 265−266.

Perutz, M. F. (1968) *J. Cryst. Growth 2*, 54−56.

Perutz, M. F., & Mathews, F. S. (1966) *J. Mol. Biol. 21*, 199−202.

Potter, W. T., Hazzard, J. H., Choc, M. G., Tucker, M. P., & Caughey, W. S. (1990) *Biochemistry 29*, 6283−6295.

Rohlfs, R. J., Mathews, A. J., Carver, T. E., Olson, J. S., Springer, B. A., Egeberg, K. D., & Sligar, S. G. (1990) *J. Biol. Chem. 265*, 3168−3176.

Satow, Y., Cohen, G. H., Padlan, E. A., & David D. R. (1986) *J. Mol. Biol. 190*, 593−604.

Shaanan, B. (1983) *J. Mol. Biol. 171*, 31−59.

Shen, T.-J., Ho, N. T., Simplaceanu, V., Zou, M., Green, B. N., Tam, M. F., & Ho, C. (1993) *Proc. Natl. Acad. Sci. U.S.A. 90*, 8108−8112.

Smerdon, S. J., Dodson, G. G., Wilkinson, A. J., Gibson, Q. H., Blackmore, R. S., Carver, T. E., & Olson, J. S. (1991) *Biochemistry 30*, 6252−6260.

Springer, B. A., Egeberg, Sligar, S. G., Rohlfs, R. J., Mathews, A. J., & Olson, J. S. (1989) *J. Biol. Chem. 264*, 3057−3060.

Tame, J., Shih, D. T.-b., Pagnier, J., Fermi, G., & Nagai, K. (1991) *J. Mol. Biol. 218*, 761−767.

Yanase, H., Cahill, S., de Llano, J. J. M., Manning, L. R., Schneider, K., Chait, B. T., Vandegriff, K. D., Winslow, R. M., & Manning, J. M. (1994) *Protein Sci. 3*, 1213−1223.

BI9519967